



**HAL**  
open science

## Optical optimization of semi-transparent a-Si:H solar cells for photobioreactor application

A. Brodu, C. Seydoux, G. Finazzi, C. Dublanche-Tixier, C. Ducros

► **To cite this version:**

A. Brodu, C. Seydoux, G. Finazzi, C. Dublanche-Tixier, C. Ducros. Optical optimization of semi-transparent a-Si:H solar cells for photobioreactor application. *Thin Solid Films*, 2019, 689, pp.137492. 10.1016/j.tsf.2019.137492 . hal-02332917

**HAL Id: hal-02332917**

**<https://hal.science/hal-02332917v1>**

Submitted on 29 Sep 2020

**HAL** is a multi-disciplinary open access archive for the deposit and dissemination of scientific research documents, whether they are published or not. The documents may come from teaching and research institutions in France or abroad, or from public or private research centers.

L'archive ouverte pluridisciplinaire **HAL**, est destinée au dépôt et à la diffusion de documents scientifiques de niveau recherche, publiés ou non, émanant des établissements d'enseignement et de recherche français ou étrangers, des laboratoires publics ou privés.

# Optical optimization of semi-transparent a-Si:H solar cells for photobioreactor application

**Authors:** A. BRODU<sup>\*a</sup>, C. SEYDOUX<sup>c</sup>, G. FINAZZI<sup>c</sup>, C. DUBLANCHE-TIXIER<sup>b</sup>, C. DUCROS<sup>a</sup>

\* Corresponding author

CEA-LITEN-DTNM, 17 rue des martyrs 38054 GRENOBLE Cedex 9

Email: [agathe.brodu@cea.fr](mailto:agathe.brodu@cea.fr)

Tel: +33 4 38 78 08 76

- a. Univ. Grenoble Alpes, CEA, LITEN, DTNM, LCH, 17 rue des martyrs 38054 GRENOBLE Cedex 9, France.
- b. Univ. Limoges, IRCER, UMR 7315, 16 rue Atlantis, 87068 Limoges cedex, France
- c. Université Grenoble Alpes (UGA), Centre National de la Recherche Scientifique (CNRS), Commissariat à l'Énergie Atomique et aux Énergies Alternatives (CEA), Institut National de la Recherche Agronomique (INRA), Laboratoire de Physiologie Cellulaire et Végétale, UMR 5168, Institut de Biosciences et Biotechnologie de Grenoble (BIG), CEA-Grenoble, 17 rue des martyrs 38054 GRENOBLE Cedex 9, France

**Keywords.** Photobioreactor, Phaeodactylum Tricornutum, Hydrogenated amorphous silicon solar cell, Textured substrate, Antireflective texture, Light scattering texture, Reactive ion etching

**Abstract.** To improve the overall photoconversion efficiency and provide energy support for microalgae culture, we propose to develop a photobioreactor (PBR) and

photovoltaic technology (PV) coupled system using a-Si:H solar cells directly placed on the PBR's illuminated surface.

PV cells have to absorb a part of the incident light to produce electricity while being transparent in the photosynthesis wavelength range. Growing test of *Phaeodactylum Tricornutum* shows that PV optical filtering does not influence the growth rate. Optical modifications of solar cells layers thicknesses and reactive ion etching of the glass substrate applied to very thin solar cells allowed to maintain a high PV efficiency while maintaining the growth rate of microalgae.

The antireflection texture, combined with a light scattering effect applied on the upper side of the substrate gives the best results. Short circuit current of thin solar cells goes from 7.3 to 10.2 mA/cm<sup>2</sup>, and the efficiency increased from 3.5 to 4.7 %.

## 1. Introduction

Microalgae are a diverse group of eukaryotic organisms, with 30 000 listed species, estimated to 1 million species in total [1]. Depending on the species, microalgae grow in a wide range of habitats like fresh, brackish or marine waters with polar to tropical temperatures. Their sizes go from one micrometer to a hundred. Today, these microalgae are used: (i) as carbon sink to absorb the CO<sub>2</sub> even not pure from the atmosphere [2], (ii) to produce a high-efficiency 3rd generation of biofuels and biogas [3], (iii) to filter wastewaters, soils and flue gases from various industries [4], (iv) to produce high-value compounds, such as phycocyanin, carotenoids and fatty acids used in many applications [5]. For those applications, the market is up-and-coming, meeting a vital and environmental need, and that is why it faces growing demands. The industrialization of microalgae products requires a highly productive closed-culture system called photobioreactor (PBR) [6]. However, industrial-scale production is mainly limited by the low efficiency to convert sunlight into biomass.

A small range of the full spectral bandwidth of light reaching the PBR surface is used to produce biomass [7]. The importance of wavelengths received by microalgae has been demonstrated by Kim et al. [8]. They highlighted the impact of blue wavelengths on the microalgae size and red wavelengths on their cells division. However, the low efficiency of sunlight conversion is also linked to the irradiance received by the microalgae culture. There are several factors like light energy or also the overall photon flux density. If they are too high, microalgae can reach a light saturation point, called photo-inhibition, which stresses and could even damage the culture. On the other hand, if the light energy is too low, the infrared radiations raise the PBR temperature and damage the culture. The culture in photobioreactor is also

limited by the energy consumption needed to regulate and control the temperature, the homogenization, and the biotechnologically important parameters.

To optimize the light received by the PBR and bring a power supply, it is possible to combine a photovoltaic (PV) technology with a photobioreactor on the same surface to exploit all the incident solar spectrum [9]. As mentioned previously, microalgae only require 400-550 nm and 650-700 nm wavelength parts of the visible solar spectrum, whereas photovoltaic cells absorb over a large part of the spectrum, depending on the technology. This way, Sforza et al. [10] proposed to cover one-third of the PBR irradiated surface with opaque silicon photovoltaic cells. This system has a higher photoconversion efficiency while reducing photo-inhibition under high light intensities. In the same objective, the *Purple Sun* project [11] built a Microalga Photovoltaic Greenhouse of 60 m<sup>2</sup>. This system offers high efficiency at reduced costs with a semi-transparent a-Si PV panel from Sunpartner coupled with a new solar tracker. Going further, Barbera et al. [12] described an integration of semi-transparent dye-sensitized solar cells deposited directly on the photobioreactor irradiated surface. Results showed that under day-night irradiation, productivity remains the same. Finally, the presence of the PV system does not affect either the biomass productivity or the algae pigment content.

The objective of this study was to combine a semi-transparent photovoltaic hydrogenated amorphous silicon (a-Si:H) based technology and a photobioreactor. Such technology is low cost, mature, with low processing temperature but high-temperature resistance. Moreover, amorphous silicon absorbs the light in a complementary range of PBR: 350-750 nm with maximum absorption at 500 nm. Both semi-transparency and PV efficiency of these solar cells can be optimized. Figure 1 presents the schematic view of our PBR/PV coupled system. We first investigated if

our PV/PBR coupled system could convert a large part of the incident solar spectrum without lowering the PBR efficiency. Then, we optically optimized the a-Si:H photovoltaic cells by changing the thicknesses of the layers. These PV cells had to be semi-transparent to transmit a maximum of sunlight to PBR in order to keep a sufficient microalgae culture rate. To maintain a good optical solar transmission while keeping a sufficient electrical efficiency, we also proposed to optimize optically the substrate of the solar cells by texturing.

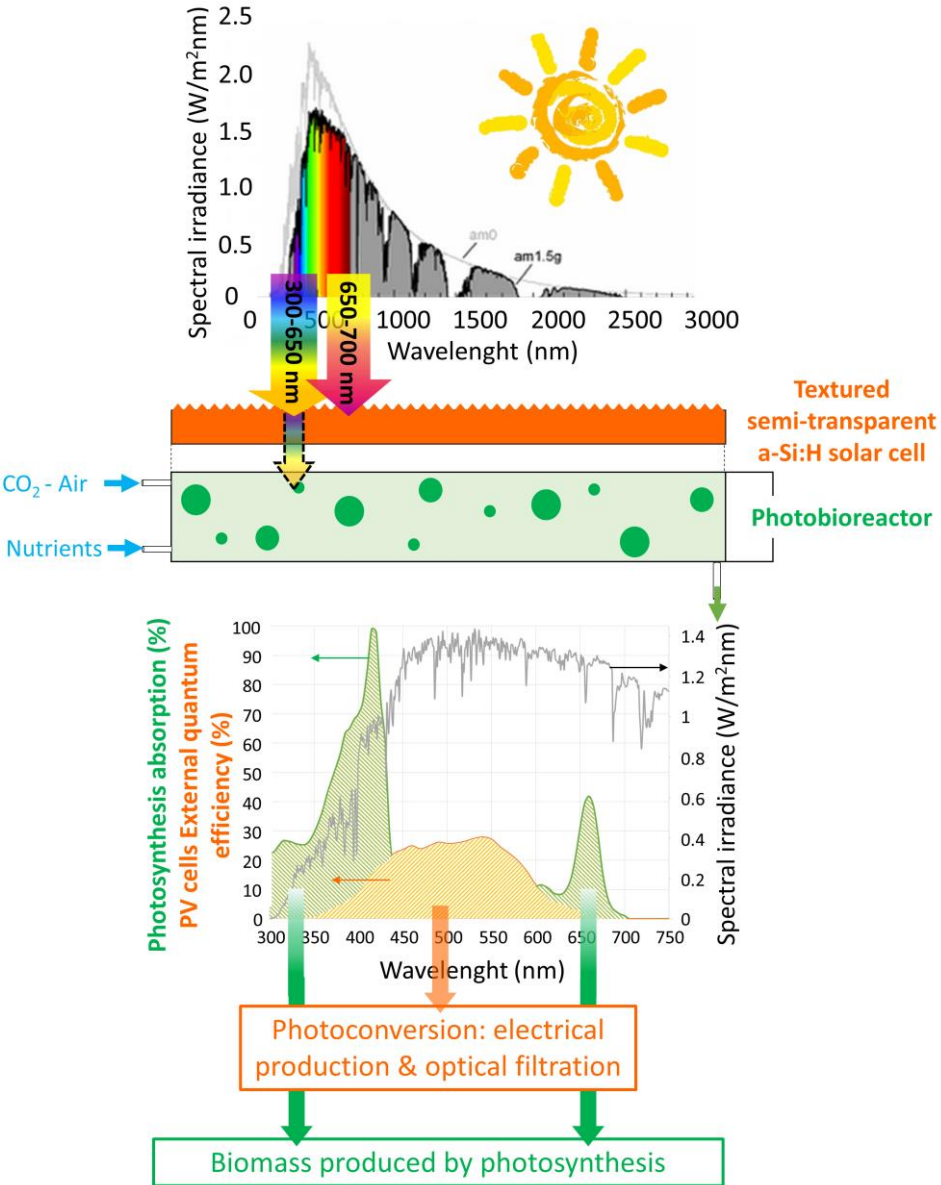


Figure 1. Schematic of the PBR/Semi-transparent thin film solar cell coupled system.

## **2. Materials and methods**

### **2.1. Texturing process**

A random and controlled textured surface (shape, period, and height) was obtained by reactive ion etching (RIE) using Nextral NE110 equipment. A radio frequency (RF) polarization was applied to the upper electrode. The substrate holder was grounded. Reactive chemical gas was a mixture of  $\text{CHF}_3$  and  $\text{O}_2$ .

The morphological properties of textured surfaces were characterized by scanning electron microscopy (SEM) (LEO Gemini 1530) with an accelerating voltage of 5.0 kV, a working distance between 6.6 and 6.9 mm and a magnification of 50.0 (figure 5) and 15.0 kX (figure 8).

### **2.2. Hydrogenated amorphous silicon (a-Si:H) based solar cells**

The structure of the a-Si:H solar cells elaborated in this study is a (Corning Eagle Xg glass/ZnO:Al/a-Si:H p-i-n /ZnO:Al/metallic back contact) configuration.

The transparent conductive oxide (TCO), ZnO:Al (AZO) coating was elaborated by RF magnetron sputtering from a pure AZO target (purity of 99.99 % with 2 wt% of  $\text{Al}_2\text{O}_3$  dopant).

Hydrogenated amorphous silicon layers were deposited in a single deposition chamber. Doped layers (boron and phosphorus-doped a-Si:H) and intrinsic a-Si:H layer were elaborated using a Plasma-Enhanced Chemical Vapor Deposition. The gases precursors are silane ( $\text{SiH}_4$ ), hydrogen ( $\text{H}_2$ ), methane ( $\text{CH}_4$ ), trimethylboron for the boron doped layer (p-layer) and phosphine ( $\text{PH}_3$ ) for the phosphorus-doped layer (n layer). The deposition temperature was kept at 200°C following literature optimum [13].

A silver of metallic contact was deposited on the back TCO to collect the charge carriers.

Sixteen 4x4 mm<sup>2</sup> PV cells were elaborated on a 25x25 mm<sup>2</sup> Corning glass for electrical characterization. 50x50 mm<sup>2</sup> Corning glass substrates were coated with the same stack to perform optical characterization. These large surface samples were also used as optical filters in order to evaluate their performances during microalgae growth rate tests.

Solar cells layers thicknesses were adjusted using optical simulation software (Optilayer, Version 12.12, Optilayer GmbH). These thicknesses are measured using spectroscopic ellipsometry (Semilab SE 2100). For the AZO thicknesses, a combined Tauc-Lorentz and Drude models are used [14]. The thickness of amorphous silicon layers (intrinsic and doped) was analyzed using a Tauc-Lorentz model [14].

### **2.3. Electrical characterization**

External quantum efficiency (EQE) measurements were carried out in a ReRa Spequest setup. The EQE curve was given at short circuit condition without any bias (optical or electrical). Current density-voltage (J-V) measurements also characterized the solar cells under AM1.5 illumination in standard conditions (25°C, 100 mW/cm<sup>2</sup>) with a SpectraNova sun simulator. From these J(V) curves, the open-circuit voltage (Voc), the short circuit current density (Jsc) and the Fill Factor (FF) were measured.

### **2.4. Optical characterization**

The total reflectance (Rt), the total transmittance (Tt) and the diffuse transmittance (Td) of solar cells were measured in a 250-1100 nm spectral range using a Perkin Elmer Lambda 950 spectrophotometer with an integrating sphere (diameter 150 mm). The absorbance (At) was then deduced from equation 1:

$$A_t + R_t + T_t = 100$$

Equation 1

Thereafter, the semi-transparency percentage ( $C_{ST}$ ) was calculated following equation 2. This criterion is determined over the photosynthesis absorption wavelength range (400-750 nm), according to the solar spectrum AM 1.5 ( $W.m^{-2}.nm^{-1}$ ) and the *Phaeodactylum tricornutum* absorption spectrum ( $A_{PT}$ ):

$$C_{ST}(\%) = \frac{\int_{400}^{750} AM1.5 \text{ spectrum} \times Tt (\%) \times A_{PT}}{\int_{400}^{750} AM1.5 \times A_{PT}} \quad \text{Equation 2}$$

By the same approach, the light scattering ( $C_D$ ) percentage is calculated by replacing Tt by Td.

## 2.5. Algae strains and culture media

A-Si:H solar cells were tested on a microalgae culture of *Phaeodactylum tricornutum*, and their influence as optical filters on microalgae growth rate were evaluated. The Pt1 *Phaeodactylum tricornutum* strain (CCAP 1055/3) was obtained from the Culture Collection of Algae and Protozoa, Scottish Marine Institute (UK). The culture was grown in a beaker of ESAW (Enriched Seawater, Artificial Water) medium with 110 rpm shaking for a culture volume of 10 ml at 23°C without any input of nutrient or carbon dioxide during the growth. This system is insulated from the outside contaminations and stray light with foil. Cells ( $5 \times 10^5 \text{ cells.ml}^{-1}$ ) were exposed to a white light illumination to run a specific microalgae growth rate test. Half of the flasks were placed over a solar cell optical filter; the other half were directly placed over the light panel. A quantitherm light sensor (QRT1, Hansatech) adjusted the irradiance to obtain a light intensity of  $20 \mu\text{mol photon.s}^{-1}.m^{-2}$  for both filtering and reference samples. The experiment was performed in biological triplicates. The algae growth rate was deduced from the number of cells in a 15  $\mu\text{L}$  sample, using an automated cell counter (Luna

Automated Cell Counter, Logos Biosystems). The specific growth rate of the microalgae was calculated using equation 3:

$$\mu = \frac{\ln(N_2 - N_1)}{(t_2 - t_1)} \quad \text{Equation 3}$$

Where  $\mu$  is the specific growth rate, and  $N_1$  and  $N_2$  are the biomass ( $10^6$  cells/mL) at time 1,  $t_1$  and time 2,  $t_2$  (hour), respectively.

### 3. Results and discussion

#### 3.1. Evaluation of the PV/PBR coupled system

As solar cell filtering changed the amount of light received by the microalgae culture, it is important to evaluate the impact of such optical filtering on the microalgae growth rate. A standard semi-transparent solar cell, without any optical optimization, was used to run this test. It was composed of (Corning Eagle Xg glass/AZO front, 280 nm/a-Si:H p-i-n, 205 nm /AZO back, 265 nm). Figure 2 shows the absorption spectrum of a *Phaeodactylum tricornutum* (PT) culture and the total transmission through the standard semi-transparent a-Si:H solar cell ( $C_{ST} = 21.2\%$ , efficiency = 4.1 %), measured by spectrophotometry. It is notable that the solar cell does not transmit light between 400 and 550 nm, which is the range of the first absorption peak of the *Phaeodactylum tricornutum*.

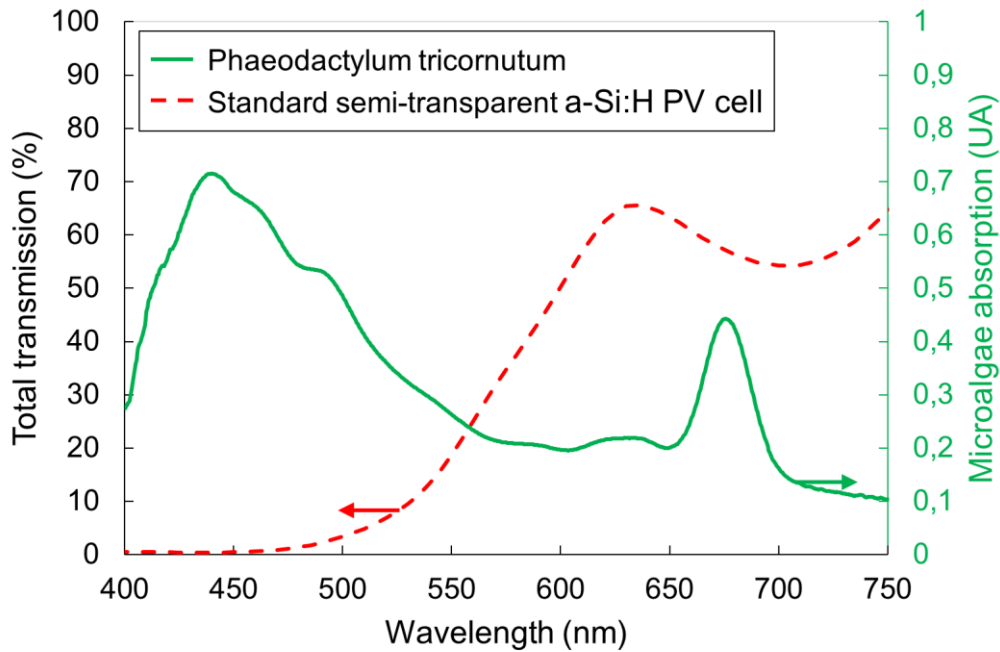


Figure 2. Absorption spectrum of a *Phaeodactylum tricornutum* culture and total transmission spectra through a semi-transparent a-Si:H solar cell.

To investigate whether this peak masking influences the microalgae growth rate, two samples were compared (figure 3): a reference sample (Corning glass only) and a test sample (Corning glass with semi-transparent PV cell masking as described in figure 1). It can be observed that both growth curves present the same two phases [15]:

- 0–225 h: an exponential acceleration phase corresponding to the division of each cell into two cells (see the inset in figure 3). The microalgae specific growth rate during this period is  $0.02 \text{ h}^{-1}$  with and without an optical filter (Eq. 3).
- 225–275 h: a stationary phase that depicts a stabilized concentration. This stabilization traduces a standard phenomenon for this type of growing test: one of the essential elements is missing (nitrogen, phosphorus, carbon), so the growth rate decreases and just compensate the cells mortality.

In this first part, we demonstrated that semi-transparent a-Si:H PV cells set in front of PBR did not affect the *Phaeodactylum tricornutum* growth rate even if it wholly filtered a large amount of light necessary for its growth (400–550 nm). This result has

been observed in other studies [16,17]. Nevertheless, photovoltaic devices had to be improved in order to enhance their semi-transparency and efficiency.

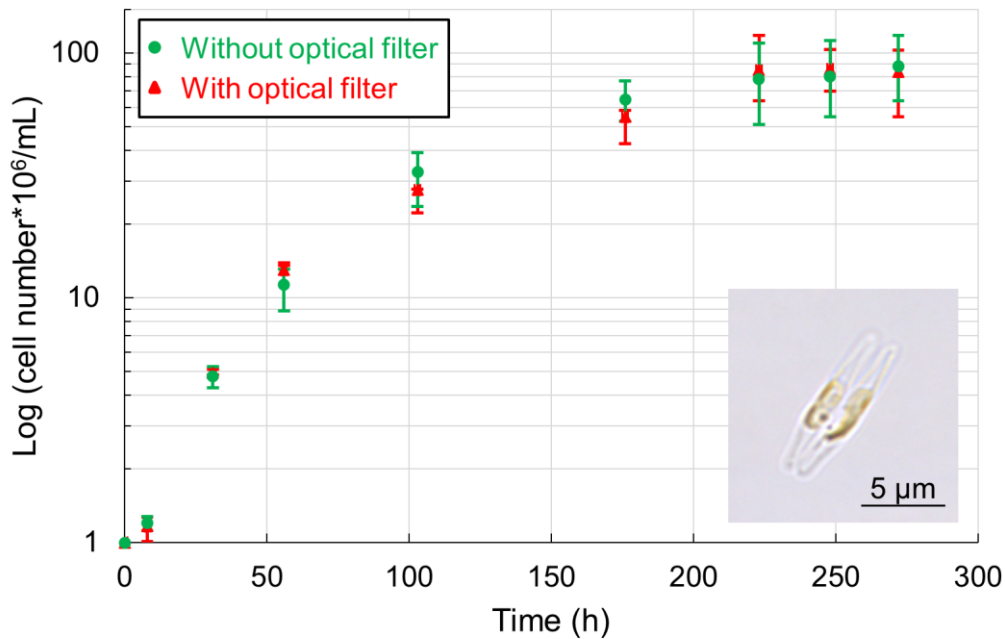


Figure 3. Growth rate of a *Phaeodactylum tricornutum* with and without a-Si:H cell optical filter and inset, a microscope picture of a cell division.

### 3.2. Optimization of the PV cell semi-transparency

Each layers thickness of the solar cell was adjusted to enhance the PV cell semi-transparency as a function of microalgae spectral response. Concerning AZO thicknesses, the target was to achieve the best compromise between optical properties (high transmittance in the 400–1100 nm spectral range) and low resistivity (i.e., below  $1 \cdot 10^{-3}$  ohm.cm) in order to collect the charge carriers generated by amorphous silicon. Concerning amorphous silicon layers (p doped, intrinsic and n doped), the target was to improve the transparency of the solar cell while keeping sufficient optical absorption of photons to generate electrical carriers. According to the optical simulation, the optimized solar cell was composed of (Corning Eagle Xg glass/AZO front, 250 nm/a-Si:H p-i-n, 240 nm /AZO back, 250 nm). Figure 4 describes the total transmission of this optimized semi-transparent solar cell and that of the standard semi-transparent

solar cell used in the previous growth study. The transmission was enhanced in the 600–700 nm wavelength range. A  $C_{ST}$  of 22.5 % (Eq. 2) is measured for this optimized semi-transparent (ST) solar cell compared to the standard one (21.2 %).

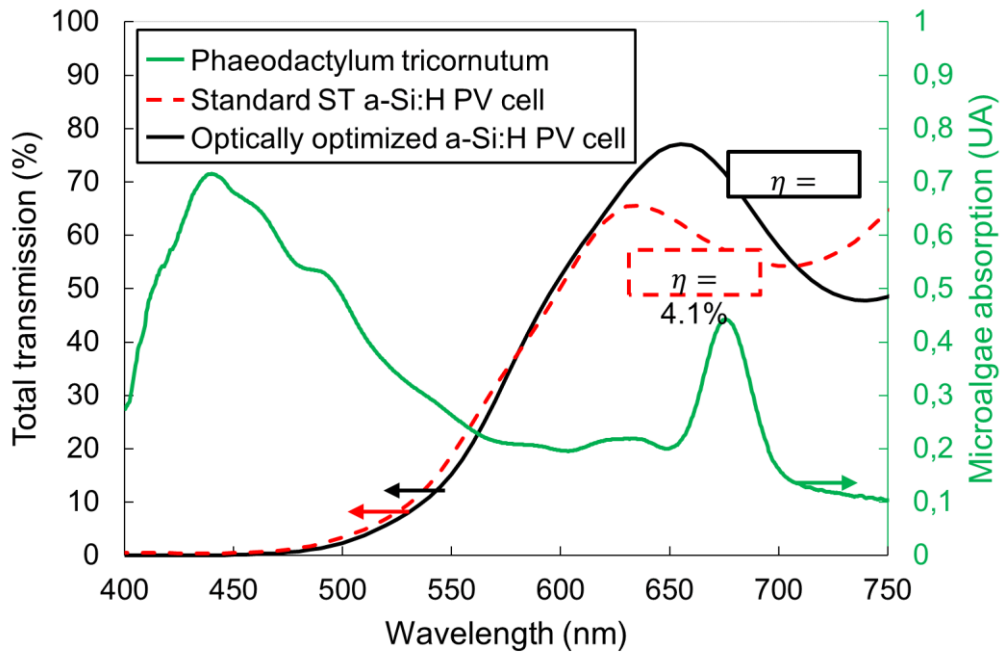


Figure 4. Absorption spectrum of a *Phaeodactylum tricornutum* culture, total transmission spectra through a semi-transparent a-Si:H solar cell before and after optical optimization.

However, because of the modification of AZO and amorphous silicon thicknesses, the PV efficiency was reduced from 4.1 % to 3.5 %. This low efficiency was mainly due to (i) a low absorption of photons in amorphous silicon due to its low thicknesses (ii) a bad collection of charge carriers in AZO due to its high resistivity ( $R_{\square} = 40 \text{ } (\Omega/\square)$ ). Many authors [18–21] proposed to improve the absorption of photons in thin amorphous silicon solar cells by inserting light scattering surfaces. Other studies [22–24] indicated the impact of antireflective texturing to improve current density. Therefore, we proposed to improve the semi-transparent solar cell efficiency by: (i) increasing the front AZO thickness in order to increase its conductivity (ii) inserting optical interfaces by texturing the substrate. This texturing could act as a light scattering or antireflective surface as described in the following part.

The glass substrate was textured by RIE. This process involves two distinct etching mechanisms, an ion bombardment and a chemical attack. The final shape of the texture depends on the  $\text{CHF}_3$  and  $\text{O}_2$  gas flow rates, the pressure in the chamber, the RF power, and the process time [25,26]. A design of experiments was used in order to sweep the experimental domain with equal distribution. Three main groups of texturing were evidenced; the working parameters are indicated in table 1.

Table 1. RIE working parameters for the different textured surfaces.

	$\text{CHF}_3$ flow	$\text{O}_2$ flow	Pressure	RF Power	Time
	(sccm)	(sccm)	(mTorr)	(W)	(s)
Texture 1	13	2	120	200	400
Texture 2	15	0	160	150	3000
Texture 3	25	8	195	250	3600

The surface morphology of these three groups was observed by scanning electron microscopy (figure 5). Texture 1 (Fig. 5a) is the smallest design obtained (height~100 nm; width~70 nm). Texture 3 (Fig. 5c) is the most prominent design (height~650 nm; width~450 nm). An intermediate texture, texture 2 (Fig 5b) displays the medium size of random pyramids (height~200 nm; width~100 nm).

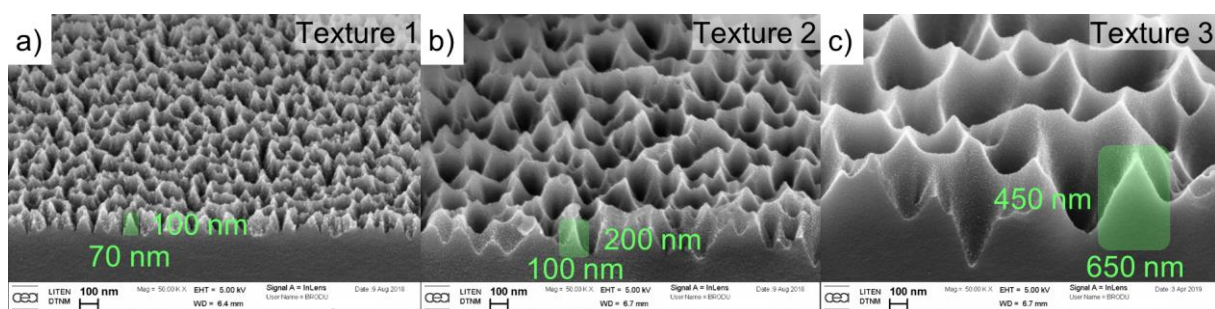
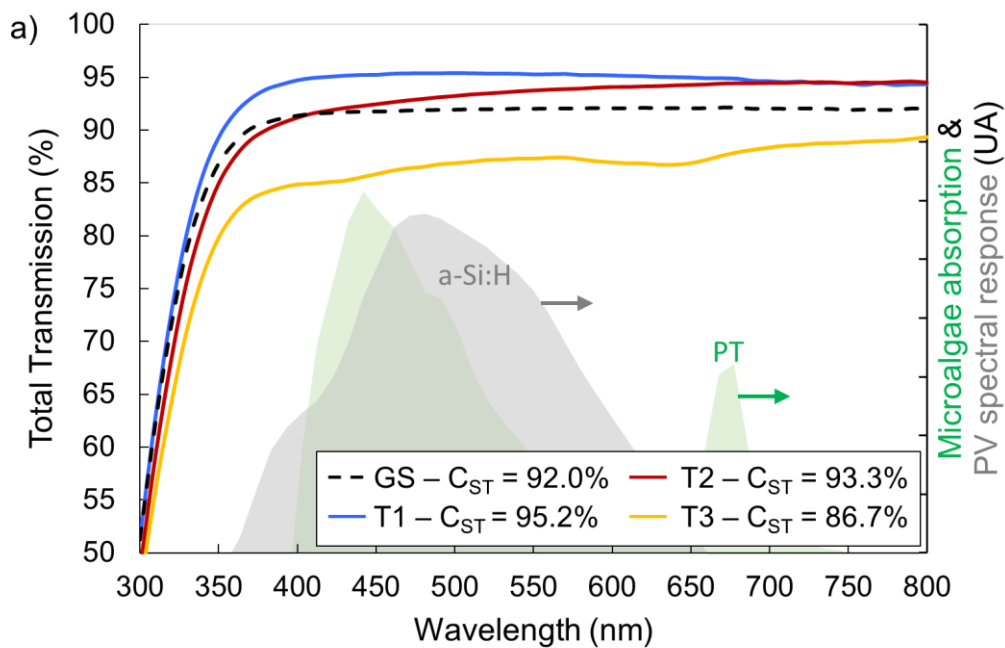


Figure 5. SEM images of textured glass a) 1 b) 2 c) 3 at the same magnification.

The total and diffuse transmittance of the three textured glasses were compared with a Corning Eagle Xg glass (figure 6).  $C_{ST}$  and  $C_D$ , calculated from the spectrophotometry curves (Eq. 2) were also listed in figure 6. Texture 1 presents the

best total transmission ( $C_{ST} = 95.2\%$ ) without any light diffusion ( $C_D = 0.1\%$ ). This thin pattern and its shape were similar to antireflective textures obtained with the same RIE process and detailed in the literature [27–29]. It limits Fresnel losses due to reflection at the glass-air interface thanks to a gradual transition of its refractive index. Texture 3 has the highest diffusion criterion ( $C_D = 59.2\%$ ) and the lower semi-transparency property ( $C_{ST} = 86.7\%$ ). This texture with high diffuse transmission is mainly used for scattering incident solar light into the solar cell in order to increase the optical path of the photons [30–32]. Texture 2 is an intermediate texture between Texture 1 and 3: it combined both enhancements with a  $C_{ST}$  of 93.3% and a  $C_D$  of 3.2%. Finally, it should be noted that both antireflective and light scattering textures could be obtained with the same technology, the reactive ion etching.



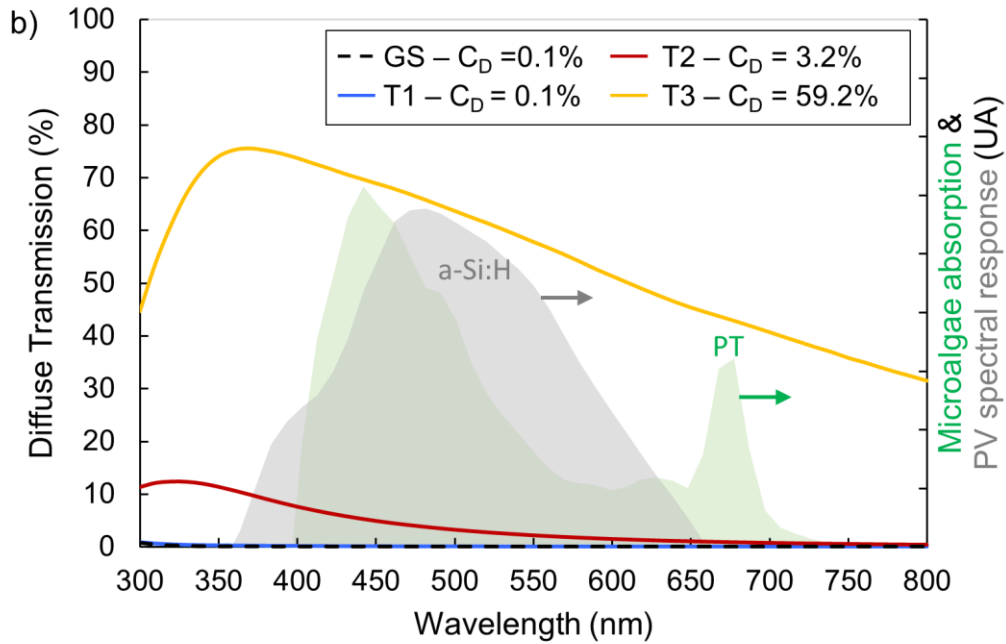


Figure 6. a) Total and b) diffuse transmission of the glass substrate (GS) and textured glass 1 (T1), 2 (T2) and 3 (T3) compared with the *Phaeodactylum tricornutum* (PT) absorption and the hydrogenated amorphous silicon (a-Si:H) cell spectral response.

### 3.3. Characterization of textured solar cells

These different textured glass substrates were used to apply semi-transparent solar cells in a superstrate configuration (figure 7). Figure 7a describes the solar cell without any textured surface (Reference). Antireflective textures, texture 1 and 2, were applied on the upper side (Fig. 7b) and named T1US and T2US, respectively. Light scattering textures, texture 2 and 3, were applied on the backside (Fig. 7c) and respectively named T2BS and T3BS.

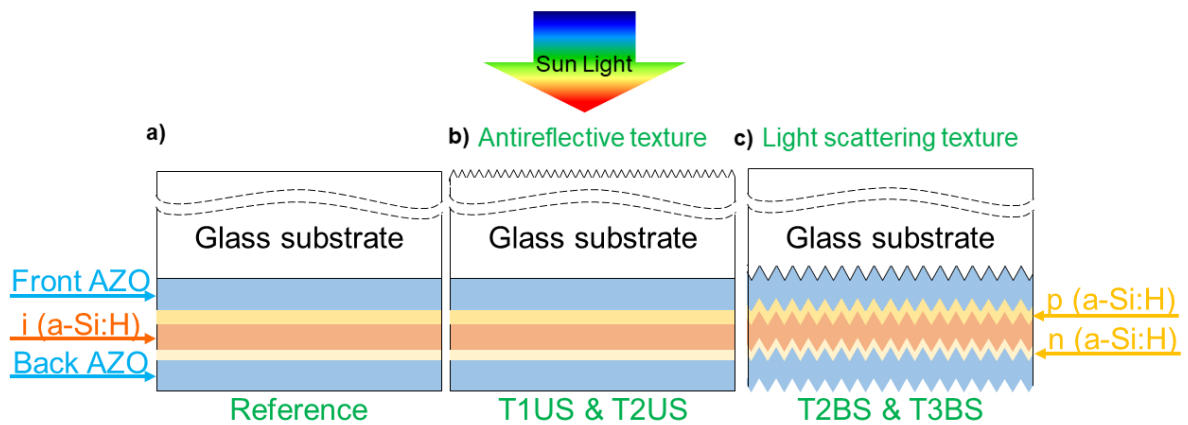


Figure 7. Solar cells configuration with a) reference glass b) antireflective glass and c) light scattering glass.

Figure 8 shows SEM cross-section images of the reference solar cell without any textured surface (Fig. 8a) and the backside textured solar cells (T2BS, Fig. 8b, and T3BS, Fig. 8c). It is important to note that the textured surface applied on the back side had a strong influence on all interfaces of solar cells layers: AZO growth follows the shape of the texture. Both textures (2 & 3) had an impact on AZO morphology and led to a significant decrease of the electrical conductivity.

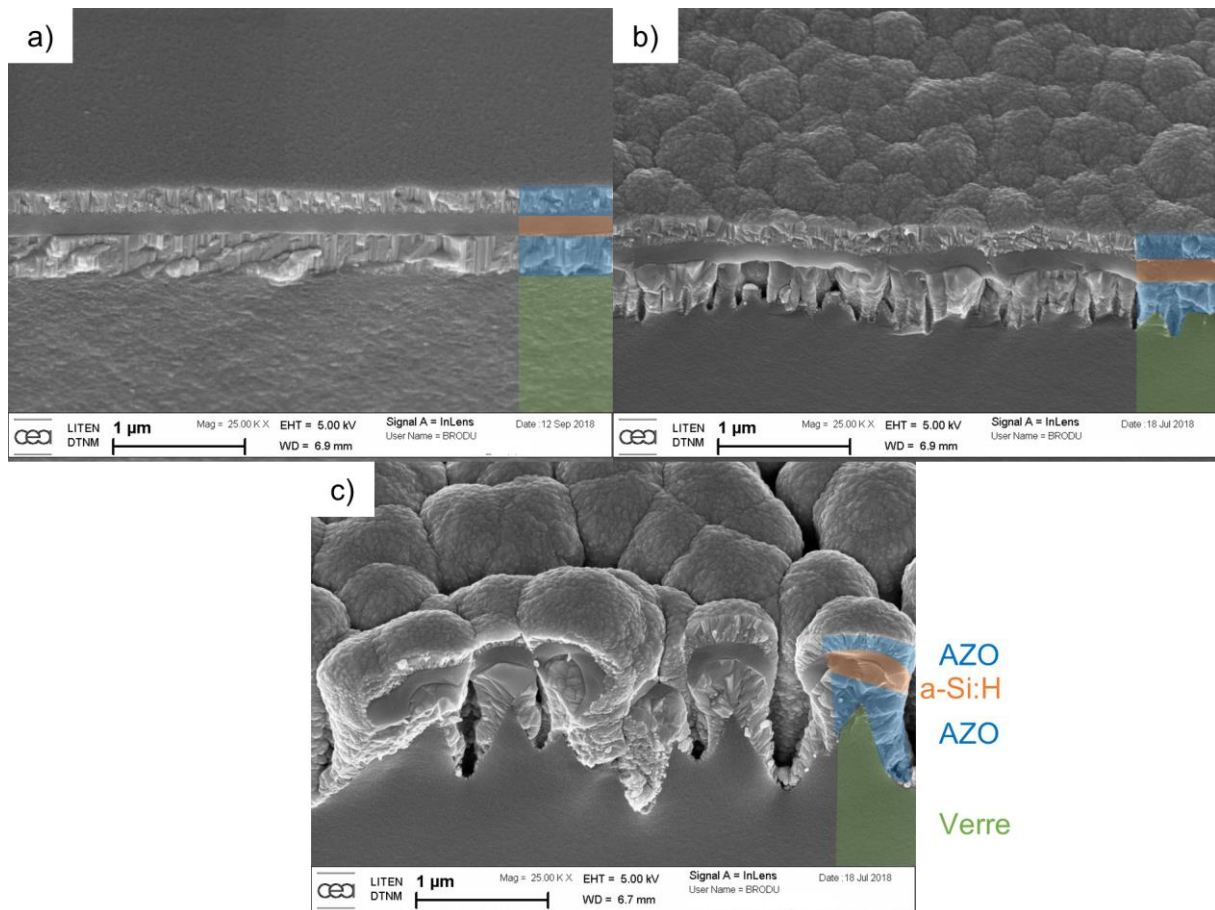


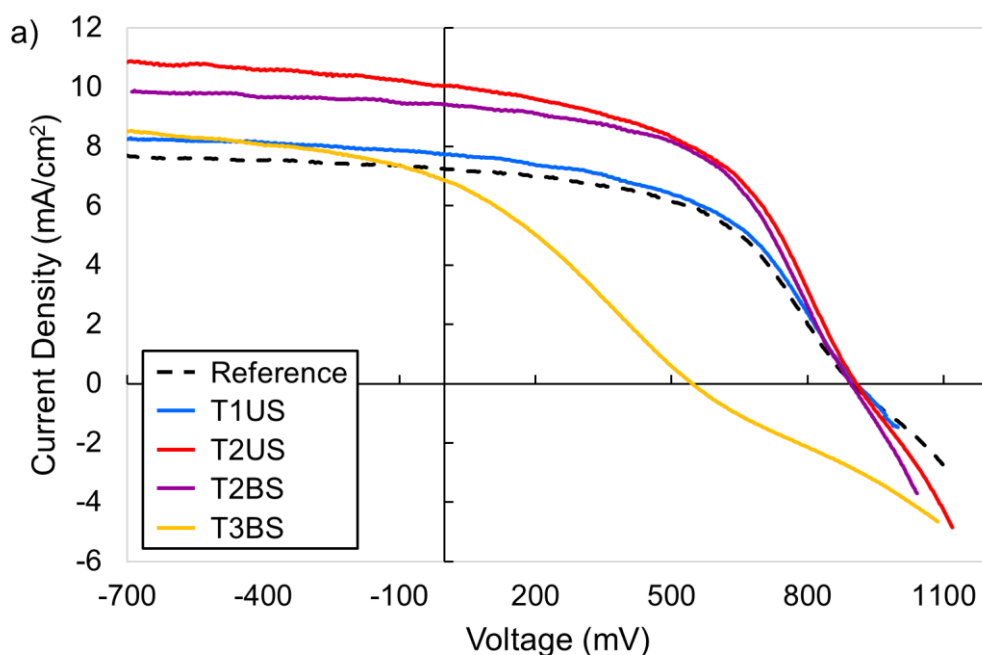
Figure 8. SEM images of solar cells a) RBS b) T2BS c) T3BS.

In order to compare only the effect of optical treatment, the electrical properties of AZO should remain constant, even on textured solar cells. We already chose in part 3.2 to increase the front AZO thickness to improve its conductivity and, as a consequence, to enhance the efficiency without damaging the semi-transparency. A value of  $R_{\square}$  at  $21 \Omega/\square$ , compatible with a good charge extraction in solar cells was defined for every front AZO by adjusting their thicknesses. Then, amorphous silicon layers were also deposited with the same thickness in order to evaluate only the influence of different textured surfaces on solar cell efficiency. Table 2 describes the five different solar cells deposited. Figure 9 compares the  $J(V)$  curves and the absorption spectra of these five solar cells. Table 3 presents their electrical characteristics. There are three distinct behaviors depending on the texturing.

Table 2. Different configurations and layers thicknesses of referent and textured solar cells.

	Texture			Substrate Side treated		AZO front		Amorphous silicon PIN	AZO Back	
	1	2	3	Upper	Back	(nm)	$R_{\square}$ ( $\Omega/\square$ )	(nm)	(nm)	$R_{\square}$ ( $\Omega/\square$ )
Ref						370	$21 \pm 1$	$238 \pm 3$	$238 \pm 3$	$41 \pm 1$
T1US	x			x		370				
T2US		x		x		370				
T2BS		x			x	365				
T3BS			x		x	500				

Texture T1US (antireflective texture) slightly improved the absorption in the solar cell (Fig. 9b), and so the short circuit current density ( $J_{sc}$ ) increased to  $7.7 \text{ mA/cm}^2$  without damaging the open-circuit voltage ( $V_{oc}$ ) and the field factor (FF). Indeed, solar cell efficiency slightly increased to 3.6 %. Figure 9b shows that T3BS (light scattering texture), induced high absorption in amorphous silicon solar cell. Nevertheless, the very low efficiency measured (1.0 %) was mainly due to a strong lowering of the fill factor (FF = 22 % in this case) comparatively to the reference cell (FF = 51 %). This was probably due to the too high aspect ratio of this textured surface: PV layers growing on such rough surface (Fig. 8c) should lead to low-quality interfaces.



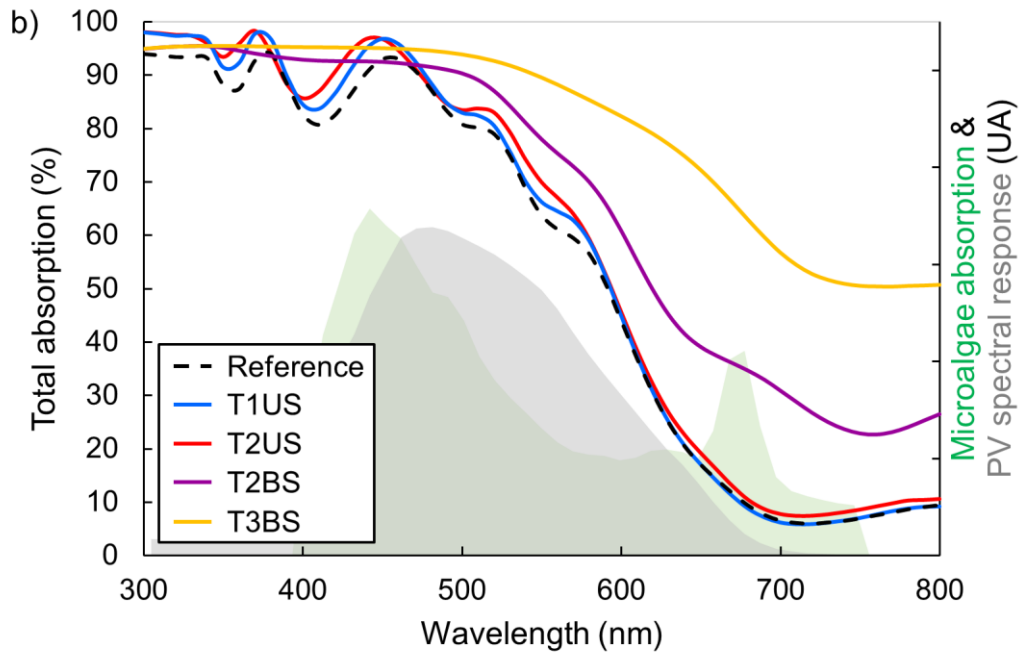


Figure 9. a)  $J(V)$  curve and b) absorption spectra of the reference T1US, T2US, T2BS and T3BS solar cells compared with the *Phaeodactylum tricornutum* (PT) absorption and the hydrogenated amorphous silicon (a-Si:H) cell spectral response

As described in table 2, texture 2 was applied on both sides of the substrate (T2US and T2BS). They both showed an enhancement of the  $J_{sc}$ , respectively 10.2 and 9.2  $\text{mA}/\text{cm}^2$  compared to the reference (7.3  $\text{mA}/\text{cm}^2$ ) while keeping the same  $V_{oc}$  and FF. Indeed, Fig. 9b shows a higher optical absorption than the reference. This texture seems to be a good compromise because the efficiencies respectively increased to 4.7 % and 4.4 % for T2US and T2BS.

Table 3. Open circuit voltage  $V_{oc}$ , short circuit current density  $J_{sc}$ , fill factor FF, and efficiency of a-Si:H pin solar cells for the different textured samples on different configurations.

	$V_{oc}$	$J_{sc}$	Efficiency	FF
	(mV)	( $\text{mA}/\text{cm}^2$ )	(%)	(%)
Ref	898	7.3	$3.5 \pm 0.1$	51
T1US	903	7.7	$3.6 \pm 0.1$	49
T2US	901	10.2	$4.7 \pm 0.2$	49
T2BS	898	9.2	$4.4 \pm 0.1$	54
T3BS	534	6.5	$1.0 \pm 0.2$	29

However, the optimization of the efficiency of semi-transparent cells must not be at the expense of their semi-transparency. Figure 10 shows the transmission spectra of the five a-Si:H solar cells and their semi-transparency percentage  $C_{ST}$ . Two different behaviors comes out according to the textured face of the substrate.

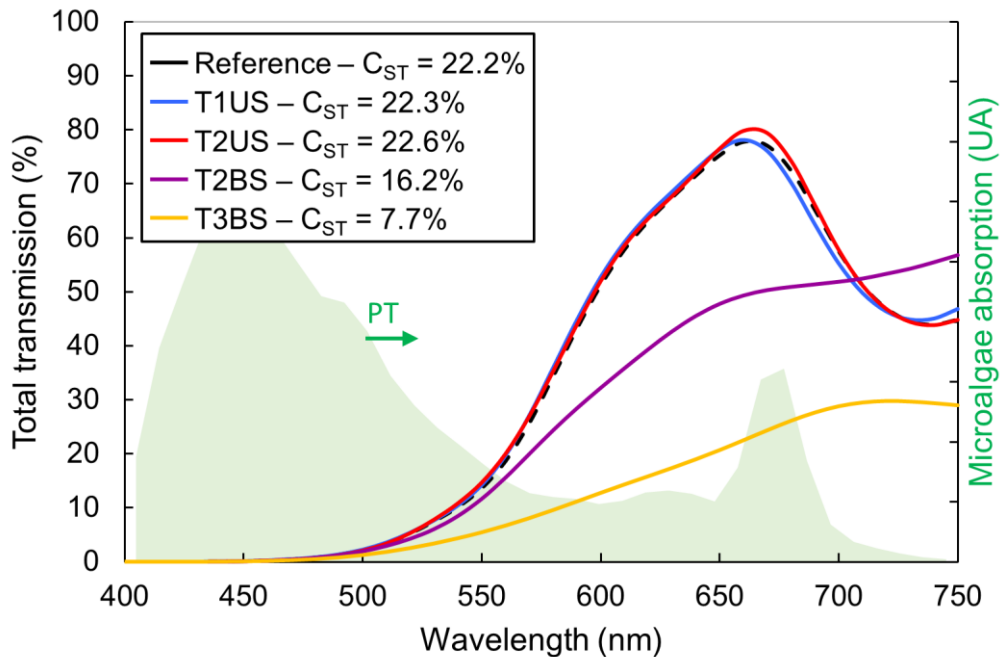


Figure 10. Transmittance spectra of textured semi-transparent a-Si:H pin solar cells compared with the microalgae *Phaeodactylum tricornutum* (PT) absorption needed.

Texturing the backside damaged the semi-transparency:  $C_{ST}$  of both T2BS and T3BS cells decreased from 22.2 % (reference) to respectively 16.2 % and 7.7 %. Fig. 9b shows that the light scattering properties of these samples contributed to increasing the light absorbance in the full range spectrum (400–1100 nm). A strong effect is notable in the interesting wavelength range needed by microalgae for photosynthesis.

On the other hand, texturing the upper side did not change the semi-transparency. That remained at around 22 % and even slightly increased to 22.6 % for T2US.

Texturing the upper side of the glass substrate with an intermediate texture 2 seems to be the best compromise. T2US achieved to enhance the efficiency from 3.5 % to 4.7 % without degrading the semi-transparency (22.6 %).

#### **4. Conclusion**

The objective of this study was to evaluate the potential coupling of an amorphous silicon photovoltaic cell with a photobioreactor. This coupled system is a viable technology to enhance the overall sunlight photoconversion efficiency and bring power supply to PBR. A semi-transparent hydrogenated amorphous silicon-based solar cell was positioned in front of the PBR.

We demonstrated that the incident sunlight optically filtered by this type of solar cell did not influence the *Phaeodactylum tricornutum* growth rate. Nevertheless, the optimization of the solar cell semi-transparency by optical simulation from 21.2 % to 22.5 % resulted in an efficiency degradation from 4.1 % to 3.5 %. To maintain a good optical solar transmission necessary to the microalgae growth rate while keeping a sufficient electrical efficiency, we optically optimized the glass substrate of the solar cell by RIE texturing. The main advantage of RIE is the possibility to obtain both an antireflective and a light scattering effects with the same process. We achieved a high semi-transparency (22.6 %) while enhancing the efficiency from 3.5 % to 4.7 % thanks to textured glass on the upper side of the superstrate solar cell.

This amorphous silicon-based solar cell could also be applied on a low temperature substrate (like polymer). Thus, we could deposit semi-transparent solar cells directly on a PBR. We could also adjust the solar cell band gap as a function of microalgae spectral response in order to optimize the use of the solar spectrum for both PV and PBR systems.

## References:

- [1] Guiry, M. D., 2012, "How Many Species of Algae Are There?," *J. Phycol.*, **48**(5), pp. 1057–1063.
- [2] Velea, S., Dragos, N., Serban, S., Ilie, L., Stalpeanu, D., Nicoara, A., and Stepan, E., 2009, "Biological Sequestration of Carbon Dioxide from Thermal Power Plant Emissions, by Absorbption in Microalgal Culture Media," *Romanian Biotechnol. Lett.*, **14**(4), pp. 4485–4500.
- [3] Moheimani, N. R., McHenry, M. P., de Boer, K., and Bahri, P. A., eds., 2015, *Biomass and Biofuels from Microalgae*, Springer International Publishing, Cham.
- [4] Udaiyappan, A. F. M., Hasan, H. A., Takriff, M. S., and Abdullah, S. R. S., 2017, "A Review of the Potentials, Challenges and Current Status of Microalgae Biomass Applications in Industrial Wastewater Treatment," *J. Water Process Eng.*, **20**, pp. 8–21.
- [5] Pulz, O., and Gross, W., 2004, "Valuable Products from Biotechnology of Microalgae," *Appl. Microbiol. Biotechnol.*, **65**(6), pp. 635–648.
- [6] Pulz, O., 2001, "Photobioreactors: Production Systems for Phototrophic Microorganisms," *Appl. Microbiol. Biotechnol.*, **57**(3), pp. 287–293.
- [7] Chisti, Y., 2013, "Constraints to Commercialization of Algal Fuels," *J. Biotechnol.*, **167**(3), pp. 201–214.
- [8] Kim, D. G., Lee, C., Park, S.-M., and Choi, Y.-E., 2014, "Manipulation of Light Wavelength at Appropriate Growth Stage to Enhance Biomass Productivity and Fatty Acid Methyl Ester Yield Using *Chlorella Vulgaris*," *Bioresour. Technol.*, **159**(Supplement C), pp. 240–248.
- [9] Moheimani, N. R., and Parlevliet, D., 2013, "Sustainable Solar Energy Conversion to Chemical and Electrical Energy," *Renew. Sustain. Energy Rev.*, **27**, pp. 494–504.
- [10] Sforza, E., Barbera, E., and Bertucco, A., 2015, "Improving the Photoconversion Efficiency: An Integrated Photovoltaic-Photobioreactor System for Microalgal Cultivation," *Algal Res.*, **10**, pp. 202–209.
- [11] Bernard, O., Suay, R., Bechet, Q., Poncet, C., Fatnassi, H., Mairet, F., Sciandra, A., Mangin, A., Coulon, D., and Boubekri, R., 2017, "The next Generation of Microalgae

Production Systems under Photovoltaic Greenhouses,” *Acta Hortic.*, (1170), pp. 921–927.

[12] Barbera, E., Sforza, E., Guidobaldi, A., Di Carlo, A., and Bertucco, A., 2017, “Integration of Dye-Sensitized Solar Cells (DSC) on Photobioreactors for Improved Photoconversion Efficiency in Microalgal Cultivation,” *Renew. Energy*, **109**, pp. 13–21.

[13] Ramanujam, J., and Verma, A., 2012, “Photovoltaic Properties of A-Si:H Films Grown by Plasma Enhanced Chemical Vapor Deposition: YangA Review,” *Mater. Express*, **2**(3), pp. 177–196.

[14] 2018, *Spectroscopic Ellipsometry for Photovoltaics*, Springer Berlin Heidelberg, New York, NY.

[15] Richmond, A., and Hu, Q., eds., 2013, *Handbook of Microalgal Culture: Applied Phycology and Biotechnology*, John Wiley & Sons, Ltd, Oxford, UK.

[16] Şimşek, G. K., and Cetin, A. K., 2017, “Effect of Different Wavelengths of Light on Growth, Pigment Content and Protein Amount of *Chlorella Vulgaris*,” *Fresenius Environ. Bull.*, **26**(12A), pp. 7974–7980.

[17] Fozer, D., Kiss, B., Lorincz, L., Szekely, E., Mizsey, P., and Nemeth, A., 2019, “Improvement of Microalgae Biomass Productivity and Subsequent Biogas Yield of Hydrothermal Gasification via Optimization of Illumination,” *Renew. Energy*, **138**, pp. 1262–1272.

[18] Zhu, K., Neale, N. R., Miedaner, A., and Frank, A. J., 2007, “Enhanced Charge-Collection Efficiencies and Light Scattering in Dye-Sensitized Solar Cells Using Oriented TiO<sub>2</sub> Nanotubes Arrays,” *Nano Lett.*, **7**(1), pp. 69–74.

[19] Zhang, Q., Dandeneau, C. S., Zhou, X., and Cao, G., 2009, “ZnO Nanostructures for Dye-Sensitized Solar Cells,” *Adv. Mater.*, **21**(41), pp. 4087–4108.

[20] Barbé, C. J., Arendse, F., Comte, P., Jirousek, M., Lenzenmann, F., Shklover, V., and Grätzel, M., 1997, “Nanocrystalline Titanium Oxide Electrodes for Photovoltaic Applications,” *J. Am. Ceram. Soc.*, **80**(12), pp. 3157–3171.

[21] Kluth, O., Rech, B., Houben, L., Wieder, S., Schöpe, G., Beneking, C., Wagner, H., Löffl, A., and Schock, H. W., 1999, “Texture Etched ZnO:Al Coated Glass Substrates for Silicon Based Thin Film Solar Cells,” *Thin Solid Films*, **351**(1–2), pp. 247–253.

[22] Sai, H., Matsui, T., Saito, K., Kondo, M., and Yoshida, I., 2015, “Photocurrent Enhancement in Thin-Film Silicon Solar Cells by Combination of Anti-Reflective Sub-

Wavelength Structures and Light-Trapping Textures,” *Prog. Photovolt. Res. Appl.*, **23**(11), pp. 1572–1580.

[23] Ulbrich, C., Gerber, A., Hermans, K., Lambertz, A., and Rau, U., 2013, “Analysis of Short Circuit Current Gains by an Anti-Reflective Textured Cover on Silicon Thin Film Solar Cells,” *Prog. Photovolt. Res. Appl.*, **21**(8), pp. 1672–1681.

[24] Yu, P., Chang, C.-H., Chiu, C.-H., Yang, C.-S., Yu, J.-C., Kuo, H.-C., Hsu, S.-H., and Chang, Y.-C., 2009, “Efficiency Enhancement of GaAs Photovoltaics Employing Antireflective Indium Tin Oxide Nanocolumns,” *Adv. Mater.*, **21**(16), pp. 1618–1621.

[25] Ye, X., Shao, T., Sun, L., Wu, J., Wang, F., He, J., Jiang, X., Wu, W.-D., and Zheng, W., 2018, “Plasma-Induced, Self-Masking, One-Step Approach to an Ultrabroadband Antireflective and Superhydrophilic Subwavelength Nanostructured Fused Silica Surface,” *ACS Appl. Mater. Interfaces*, **10**(16), pp. 13851–13859.

[26] Baker, M. D., Himmel, C. D., and May, G. S., 1995, “In-Situ Prediction of Reactive Ion Etch Endpoint Using Neural Networks,” *IEEE Trans. Compon. Packag. Manuf. Technol. Part A*, **18**(3), pp. 478–483.

[27] Hu, L., Zhao, L., and Tan, Z., 2010, “The Application of Reactive Ion Etching (RIE) in Texturing of Multicrystalline Silicon Wafers for Solar Cells,” *ECS Trans.*, **27**(1), pp. 1093–1098.

[28] Wang, S. H., Hsiao, Y. J., Fang, T. H., Ji, L. W., Lin, M. H., Kang, S. H., and Lee, Y. C., 2014, “A Textured SiO<sub>2</sub> Antireflection Layer for Efficient Organic Solar Cells,” *Surf. Topogr. Metrol. Prop.*, **2**(3), p. 035005.

[29] Zaidi, S. H., Ruby, D. S., and Gee, J. M., 2001, “Characterization of Random Reactive Ion Etched-Textured Silicon Solar Cells,” *IEEE Trans. Electron Devices*, **48**(6), pp. 1200–1206.

[30] Barugkin, C., Allen, T., Chong, T. K., White, T. P., Weber, K. J., and Catchpole, K. R., 2015, “Light Trapping Efficiency Comparison of Si Solar Cell Textures Using Spectral Photoluminescence,” *Opt. Express*, **23**(7), pp. A391–A400.

[31] Hongsingthong, A., Krajangsang, T., Limmanee, A., Sriprapha, K., Sritharathikhun, J., and Konagai, M., 2013, “Development of Textured ZnO-Coated Low-Cost Glass Substrate with Very High Haze Ratio for Silicon-Based Thin Film Solar Cells,” *Thin Solid Films*, **537**, pp. 291–295.

[32] Hussain, S. Q., Balaji, N., Kim, S., Raja, J., Ahn, S., Park, H., Le, A. H. T., Kang, J., Yi, J., and Razaq, A., 2016, “Plasma Textured Glass Surface Morphologies for

Amorphous Silicon Thin Film Solar Cells-A Review," *Trans. Electr. Electron. Mater.*, **17**(2), pp. 98–103.